Available online at www.sciencedirect.com
ScienceDirect
Medical Engineering & Physics 30 (2008) 888–895
Medical Engineering & Physics
www.elsevier.com/locate/medengphy

Radiation effects on bone architecture in mice and rats resulting from *in vivo* micro-computed tomography scanning

R. Josh Klinck [a,b], Graeme M. Campbell [a,b], Steven K. Boyd [a,b,*]

[a] *Department of Mechanical and Manufacturing Engineering, University of Calgary, Calgary, Canada*
[b] *Roger Jackson Centre for Health and Wellness Research, University of Calgary, Calgary, Canada*

Received 10 April 2007; received in revised form 12 November 2007; accepted 22 November 2007

Abstract

Recently established techniques for performing *in vivo* micro-computed tomography (micro-CT) provide the capability of monitoring bone changes in a living animal at various points in time. However, radiation exposure from repeated micro-CT scans may have an effect on skeletal growth in normal or disease-model animals. The purpose of this study is to test a high resolution (~10 μm) *in vivo* micro-CT protocol on mice and rats used for bone research to understand the impact of micro-CT radiation exposure on bone architecture.

Ovariectomy (OVX) or sham-OVX surgery was performed on groups ($n = 6$–8/group) of 12-week-old C3H/HeJ, C57BL/6J, and BALB/cByJ mice, and one strain of rat (Wistar, retired breeders). The right proximal tibiae were scanned at weekly intervals while the contralateral left limbs were not scanned until the endpoint of the protocol. Trabecular and cortical bone morphology was compared between radiated and non-radiated limbs at the endpoint to quantify the radiation effect.

No effects of radiation were observed in OVX or sham rats. Lower trabecular bone volume was observed in the radiated limbs (−8 to −20% relative to non-radiated limb) of all mice groups except sham BALB/cByJ mice and normal control C57BL/6J mice, however, the observed effects were much less than the observed effects of ovariectomy (~40–50% total bone volume reduction, depending on mouse strain), and no interactions between radiation and OVX treatment were observed ($p > 0.2$). Using an internal non-radiated control within each animal is a potential method to elucidate the effect of radiation exposure for any *in vivo* protocol. Thus, although *in vivo* micro-CT is a valuable tool for bone-related research, the impact of radiation in skeletally immature mice should be considered, particularly for strains with low bone volume at the measured site.

Keywords: *In vivo* micro-computed tomography; Radiation; Trabecular micro-architecture

1. Introduction

An approach to quantifying three-dimensional (3D) bone structure is the use of micro-computed tomography (micro-CT) which is ideally suited for measuring rat and mouse bone micro-architecture at isotropic resolutions on the order of 10 μm [1,2]. Recently, *in vivo* methods for performing micro-CT have become available through the development of new micro-CT scanners (EVS Corp., Canada; Scanco Medical, Switzerland; SkyScan, Belgium). The significant advantage of performing *in vivo* measurements is the ability to track changes in bone mass and microstructure over time within the same living subject. Each subject can also act as its own control. This is an improvement over traditional cross-sectional methods, where much time-based information can be obscured by the variability within subject groups at each separate time point.

In vivo micro-CT holds potential for improving our understanding of the complex mechanisms involved in diseases such as osteoporosis [3–6], where deterioration of bone tissue micro-architecture increases fracture risk [7,8]. Tremendous costs and significant impacts on morbidity and mortality are associated with such fractures [9–11]. The ovariectomized (OVX) rat is the most common model for osteoporosis research and has been extensively used for observing bone

* Corresponding author at: Department of Mechanical and Manufacturing Engineering, University of Calgary, 2500 University Drive, N.W., Calgary, Alberta T2N 1N4, Canada. Tel.: +1 403 220 4173; fax: +1 403 282 8406.
E-mail address: skboyd@ucalgary.ca (S.K. Boyd).

1350-4533/$ – see front matter © 2008 Published by Elsevier Ltd on behalf of IPEM.
doi:10.1016/j.medengphy.2007.11.004

loss and testing treatments for the disease [12–15]. OVX mouse models are also of significant interest [16–19], owing to the mouse genome being completely mapped and the large availability of different inbred strains with substantial variations in bone biomechanical properties and microstructure [20,21]. However, an important consideration when utilizing *in vivo* micro-CT for such studies is the potential effect of radiation on skeletal changes in the tested animals. In humans, ionizing radiation doses on the order of 3–5 Gy can induce swelling and fragmentation in growing long bones [22]. Similar doses applied to osteoblast cell cultures *in vitro* can inhibit cell proliferation and induce cell death, which could lead to impaired bone growth [23–25]. The specific effect of micro-CT induced radiation in small animals is unclear. Recent studies observed no radiation effects from *in vivo* micro-CT scanning in healthy rats and disuse mouse models of bone loss, yet there remains a lack of published data pertaining to radiation effects in ovariectomized animals and different genetic strains of mice [26,27]. There are many measurement protocols available that deliver different radiation doses, and the effects may be genetic strain, age, and site specific, thus testing all combinations would be prohibitive [21,28,29].

The purpose of this study is to test a high-resolution *in vivo* micro-CT protocol on mice and rats commonly used for bone research to understand the impact of micro-CT radiation exposure on bone, and possible interactions with ovariectomy (OVX). The methodology used is applicable to many variations of *in vivo* micro-CT protocols and will provide important baseline data for effectively designing such studies.

2. Methods and materials

Female mice from three commonly utilized inbred strains (C3H/HeJ {C3H}, C57BL/6J {BL6}, BALB/cByJ {BAL}) were subjected to OVX ($n = 7$–8 per strain) or sham–OVX ($n = 7$–8 per strain) surgery at 12 weeks of age. An *in vivo* micro-CT scanner (vivaCT 40, Scanco Medical AG, Bruetisellen, Switzerland) was used to perform measurements at the proximal tibia. Animals were under anesthesia (1.75% (v/v) isoflurane) and secured in the scanner with a custom leg holder (Scanco Medical AG, Bruetisellen, Switzerland) which allowed scanning tomographic slices in the transverse plane of the tibia. The first measurement was performed after 5 days recovery from surgery (week 0), and further measurements were performed at 1, 2, 3, and 5 weeks after the initial baseline scan. Study duration was chosen to be consistent with previous mouse OVX studies where significant effects were observed within 1 month post-surgery [28,30,31]. Groups of healthy control mice ($n = 7$ per strain) between 8 and 10 weeks of age were scanned at weeks 0, 1, 2, and 3 (measurement of controls at week 5 was not possible due to practical limitations). The right tibiae of all mice were scanned at all time points while the contralateral left limbs were used as non-radiated internal controls and were scanned only at the end of the protocol (week 5 for OVX/sham groups, week 3 for healthy controls). Scanning parameters for the mouse measurements were as follows: 10.5 μm isotropic voxel size, 55 keV voltage, 109 μA current, 200 ms integration time, 2000 projections.

The grayscale CT images were segmented using a constrained Gaussian filter (sigma = 1.2, support = 2) to remove noise, and a fixed threshold (25.5% of maximal grayscale value) was used to extract the mineralized tissue structure.

Morphological measurements, including bone volume density (BV/TV), trabecular thickness/separation/number (Tb.Th, Tb.Sp, Tb.N), and cortical thickness, cortical area, and marrow area (Ct.Th, Ct.A, Ma.A) were calculated from the resulting 3D micro-CT data for each mouse at each time point (Image Processing Language, v5.00c, Scanco Medical AG). The region of interest for analysis was the proximal tibia metaphysis. User-defined contours were outlined on every 10th slice of a 150 slice region extending 1.575 mm distally from the growth plate, starting at the point where growth plate tissue was no longer visible in the grayscale CT slice. A semi-automatic computer morphing algorithm was applied to the slices in between. The full 150 slice region was used when analyzing the trabecular bone, and the most distal 100 slices were used when analyzing the cortical bone.

A similar procedure was conducted for the rats. Female Wistar rats (retired breeders) were subject to OVX ($n = 10$) or sham–OVX ($n = 10$) surgery at approximately 8 months of age. *In vivo* micro-CT measurements of the right proximal tibia were taken after 2 days recovery from surgery (week 0) and at 2, 4, 6, 8, and 12 weeks after the baseline measurement. The contralateral limb was scanned at week 12. Study duration was chosen to be consistent with previous rat OVX studies [6,32,13]. Scanning parameters for the rat measurements were as follows: 12.5 μm isotropic voxel size, 55 keV voltage, 109 μA current, 200 ms integration time, 2000 projections. The images were Gaussian filtered (sigma = 1.2, support = 2) and thresholded (27% of maximal grayscale value). The X-ray preview image of the rat loaded in the scanner was used to identify the distal end of the tibial growth plate. User-defined contours were outlined on every 15th slice of a 211 slice region beginning at 1 mm distal from the growth plate and extending 2.45 mm distally. The 3D rat data was analyzed for the same morphological parameters as the mouse data. All scans for mice and rats were analyzed in random order with a blinded operator.

Reproducibility of the techniques used here was previously investigated by scanning and analyzing groups of 10 animals *in vivo* 4 times each within a 48 h period. The animals were awakened and repositioned after each scan. Reproducibility was high, with precision errors less than 3% in mice and less than 6% in rats for BV/TV, Tb.Th, Tb.Sp, and Tb.N (unpublished data).

Radiation dose was calculated using an ionizing chamber probe (Radcal 10X5-3CT) inside a thin-walled (0.75 mm thick) polyetherimide (PEI) tube. The PEI tube is representative of the small amount of soft tissue that shields the proximal tibia from radiation. Dose was also calculated using the same

probe in the center of the scanner gantry without the PEI tube.

Comparisons between the left and right limb within the same animal at the end of the protocol provided an indication of the radiation effect. Paired *t*-tests were used to compare left and right limbs at the endpoint, and to compare changes relative to baseline between left and right limbs within the same animal. A two-way repeated measures ANOVA was used to examine potential interactions between radiation exposure and OVX or sham surgery. Significance was noted for $p < 0.05$.

3. Results

3.1. Calculated radiation dose

Using the probe described in the previous section, the resulting radiation dose for the scanning parameters used on the mice was 712.4 mGy in the PEI tube and 845.9 mGy in air. For the scanning parameters used on the rats, the calculated dose was 502.5 mGy in the PEI tube and 596.6 mGy in air.

3.2. Radiation effect on bone morphology

3.2.1. Mice

Radiation effects are reported as average relative differences between radiated and non-radiated limbs at endpoint for all specimens within a group (Table 1). For all groups of mice, the radiated limb showed lower BV/TV, and these trends were significant ($p < 0.05$) for all groups except the sham BAL and control BL6 groups (Fig. 1).

Within the C3H strain, significant BV/TV reductions in the OVX group ($-19.4\% \pm 12.3\%$), sham group ($-10.5\% \pm 8.4\%$), and normal control groups ($-8.0\% \pm 8.0\%$) were observed.

The OVX and sham groups within the BL6 strain also had significant reductions in BV/TV ($-20.0\% \pm 15.2\%$ for OVX, $-14.0\% \pm 14.3\%$ for sham), while a similar non-significant trend was observed for the normal BL6 controls.

The normal BAL controls exhibited a significant BV/TV reduction ($-19.4\% \pm 8.6\%$) in the radiated limb relative to the contralateral limb, as did the OVX group ($-8.9\% \pm 8.0\%$). The BAL sham group displayed non-significant BV/TV reductions in the radiated limb.

Tb.Sp significantly increased in the radiated limb relative to the non-radiated limb of OVX ($14.4\% \pm 14.1\%$), sham ($14.1\% \pm 13.6\%$), and normal controls ($9.6\% \pm 10.0\%$) for the C3H strain. Similar significant increases were observed in the OVX ($18.3\% \pm 12.1\%$) and normal controls ($20.7\% \pm 9.5\%$) for the BAL strain. No significant differences in Tb.Sp were observed for the sham BAL mice or any groups of BL6 mice.

Decreased Tb.N was observed in the radiated limbs relative to non-radiated for the OVX ($-11.3\% \pm 9.2\%$) and sham

Table 1
Effect of *in vivo* radiation on trabecular and cortical bone parameters in mice and rats expressed as the mean percent difference between radiated and non-radiated limbs at endpoint[a] (S.D.)

	C3H/HeJ			C57BL/6J			BALB/cByJ			Wistar rat	
	Normal	OVX	Sham	Normal	OVX	Sham	Normal	OVX	Sham	OVX	Sham
BV/TV [mean (S.D.)]	−8.0* (8.0)	−19.4* (12.3)	−10.5* (8.4)	−13.1 (15.4)	−20.0* (15.2)	−14.0* (14.3)	−19.7* (8.6)	−8.9* (8.0)	−8.0 (11.9)	−6.5 (16.4)	1.2 (17.9)
Tb.Th [mean (S.D.)]	0.7 (1.5)	−2.6 (4.2)	−1.1 (2.3)	1.3 (5.0)	−1.2 (4.7)	−1.1 (2.3)	0.4 (6.2)	8.9* (2.4)	3.9* (2.0)	−3.1 (4.7)	2.4 (11.7)
Tb.Sp [mean (S.D.)]	9.6* (10.0)	14.4* (14.1)	14.1* (13.6)	11.3 (13.4)	13.8 (20.0)	7.8 (15.1)	20.7* (9.5)	18.3* (12.1)	12.9 (17.1)	6.8 (17.4)	4.5 (23.3)
Tb.N [mean (S.D.)]	−4.7 (9.5)	−11.3* (9.2)	−11.1* (8.5)	−9.2* (9.1)	−10.4 (13.8)	−5.5 (13.6)	−15.8* (5.4)	−14.2* (8.1)	−9.5* (10.8)	2.4 (17.1)	2.7 (19.9)
Ct.Th [mean (S.D.)]	_b_b	1.7 (2.2)	1.3 (6.1)	_b_b	3.5 (4.6)	4.8 (5.4)	_b_b	7.4* (3.3)	4.7* (2.9)	1.4 (6.5)	−0.7 (4.2)
Ct.A [mean (S.D.)]	_b_b	2.0 (2.7)	1.5 (8.2)	_b_b	1.3 (3.9)	5.7* (3.3)	_b_b	4.0 (5.2)	2.2 (2.9)	−1.3 (3.4)	−0.5 (3.7)
Ma.A [mean (S.D.)]	_b_b	−3.4* (3.8)	0.6 (8.9)	_b_b	−4.8* (4.1)	−3.6* (2.9)	_b_b	−5.7* (3.2)	−3.4 (4.6)	2.2 (6.7)	1.1 (8.3)

[a] Mean percent difference = $\sum_{i=1}^{n}[((\text{radiated}_i - \text{non radiated}_i)/\text{non radiated}_i)/n] \times 100$; n = sample number per group.
[b] Cortical bone data unavailable for mouse control groups due to computer error.
* Significant difference ($p < 0.05$) between radiated and non-radiated limbs within group.

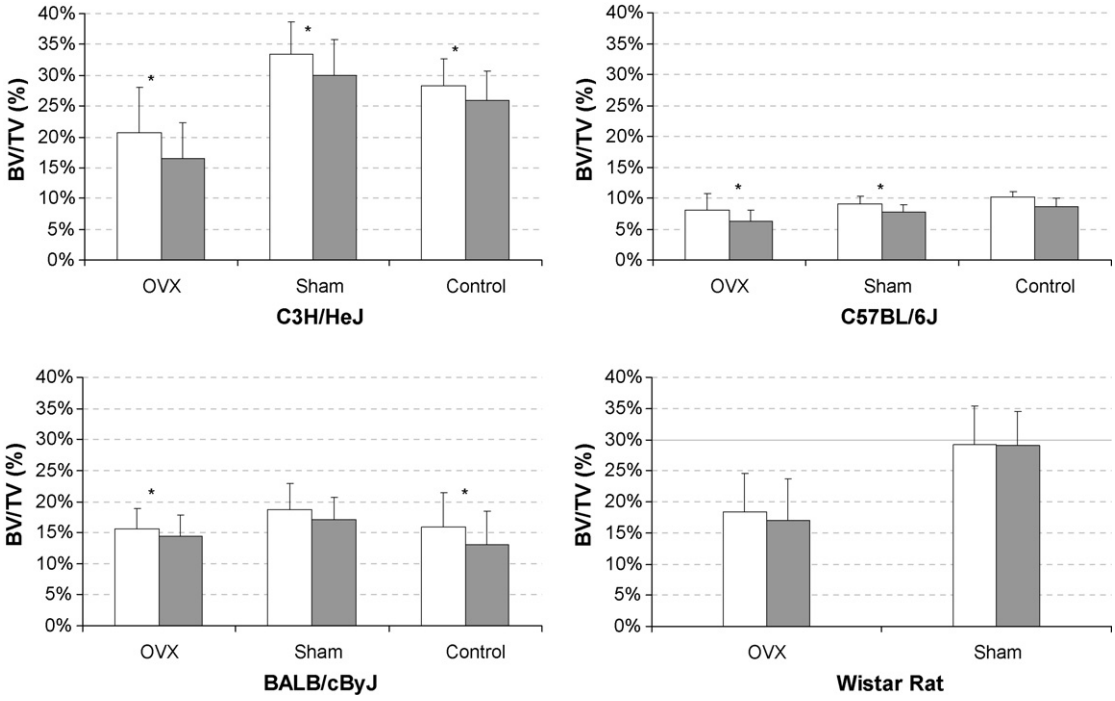

Fig. 1. Bone volume ratio for non-radiated limbs (white columns) and radiated limbs (gray columns) from all groups of C3H/HeJ, C57BL/6J, BALB/cByJ mice, and Wistar rat. OVX and sham groups compared after 5 weeks of scanning; control groups compared after 3 weeks. Asterisk indicates significant difference between irradiated and non-irradiated limbs within a group ($p < 0.05$).

($-11.1\% \pm 8.5\%$) mice for the C3H strain, as well as in normal BL6 controls ($-9.2\% \pm 9.1\%$) and in all groups of BAL mice ($-14.2\% \pm 8.1\%$ for OVX, $-9.5\% \pm 10.8\%$ for sham, $-15.8\% \pm 5.4\%$ for normal controls).

No significant differences in Tb.Th were observed between radiated and non-radiated limbs for any groups of C3H or BL6 mice, with moderate increases in the radiated limb noted only within the OVX ($8.9\% \pm 2.4\%$) and sham ($3.9\% \pm 2.0\%$) groups of BAL mice.

Ct.Th was not significantly different between radiated and non-radiated limbs for OVX or sham animals from the C3H or BL6 strains. There was, however, significantly increased Ct.Th observed in the radiated limbs relative to non-radiated for both OVX and sham groups of BAL mice ($7.4\% \pm 3.3\%$ for OVX, $4.7\% \pm 2.9\%$ for sham). Ct.A was unaffected for all mouse groups except B6 shams, which displayed significant increases in the radiated limb relative to non-radiated ($5.7\% \pm 3.3\%$). Ma.A was significantly decreased in the radiated limbs of all OVX mouse groups ($-3.4\% \pm 3.8\%$ for C3H, $-4.8\% \pm 4.1\%$ for B6, $-5.7\% \pm 3.2\%$ for BAL) and also for B6 shams ($-3.6\% \pm 2.9\%$). Cortical data was unavailable for normal control mice due to computer error.

No significant interactions between radiation and surgical treatment were observed for C3H ($p > 0.3$), BL6 ($p > 0.4$), or BAL ($p > 0.2$) mice for any morphological parameters measured. OVX was not verified by measuring uterine weight in the mice, but clear consistent patterns of bone loss were observed longitudinally within the OVX groups for each mouse strain, supporting successfulness of the procedure.

3.2.2. Rats

There were no significant differences between radiated and non-radiated limbs in either the OVX or sham rat groups for any trabecular or cortical bone morphological parameters measured (Fig. 1 and Table 1). No interaction effect between radiation and surgical treatment was observed in the rats for any parameter ($p > 0.2$). Successfulness of the OVX procedure in rats was confirmed visually by observing lack of ovarian tissue post mortem.

3.3. Longitudinal data

To put the observed effects of radiation in perspective, longitudinal morphological data for all groups is presented. Baseline values are presented along with the relative percent changes observed in the scanned and unscanned limbs at the endpoint measurement (Table 2).

The non-radiated limb of all mouse control groups showed higher BV/TV at the endpoint measurement compared to baseline, and this was significant for C3H ($21.0\% \pm 14.1\%$) and BAL ($10.0\% \pm 12.6\%$), but not BL6 ($5.9\% \pm 18.7\%$). The radiated limbs of these BAL and BL6 mice had decreased BV/TV relative to baseline ($-12.1\% \pm 11.2\%$ for BAL, $-9.9\% \pm 10.1\%$ for BL6) while radiated limbs for C3H only increased $11.1\% \pm 14.9\%$ from baseline, which is significantly less growth compared to the non-radiated limbs.

All OVX groups had significantly lower BV/TV at endpoint than at baseline, and more pronounced losses in

Table 2
Longitudinal changes in morphology for non-radiated and radiated limbs during scanning protocol

	C3H/HeJ			C57BL/6J			BALB/cByJ			Wistar rat	
	Control	OVX	Sham	Control	OVX	Sham	Control	OVX	Sham	OVX	Sham
BV/TV (%)											
Baseline	23.7 (5.4)	33.9 (3.5)	35.2 (4.4)	9.7 (1.4)	10.5 (1.2)	8.8 (0.9)	14.6 (5.4)	19.2 (2.9)	21.1 (4.3)	26.6 (7.6)	27.6 (6.0)
Δ% non-radiated	21.0 (14.1)*	−39.1 (19.8)*	−5.5 (4.7)*	5.9 (18.7)	−22.4 (28.9)	3.6 (9.9)	10.1 (12.6)*	−18.3 (13.6)*	−10.4 (14.7)	−31.5 (9.5)*	7.3 (17.2)
Δ% radiated	11.1 (14.9)	−51.4 (16.3)*	−15.5 (7.9)*	−9.9 (10.1)*	−40.0 (19.1)*	−11.4 (12.4)*	−12.1 (11.2)	−24.9 (17.7)*	−18.9 (6.2)*	−36.3 (12.5)*	6.4 (12.2)
Tb.Th (mm)											
Baseline	0.068 (0.005)	0.077 (0.004)	0.080 (0.004)	0.048 (0.002)	0.049 (0.002)	0.047 (0.002)	0.057 (0.007)	0.060 (0.003)	0.061 (0.003)	0.111 (0.009)	0.113 (0.011)
Δ% non-radiated	12.1 (4.4)*	0.4 (7.5)	8.5 (7.8)*	10.3 (5.9)*	9.6 (9.2)*	23.2 (7.8)*	6.5 (5.4)*	1.2 (7.0)	5.2 (2.8)*	1.1 (3.1)	0.9 (5.6)
Δ% radiated	12.9 (5.5)*	2.3 (7.0)	7.0 (5.1)*	11.6 (3.9)*	8.4 (11.2)	21.8 (7.0)*	6.7 (5.3)*	10.1 (8.0)*	9.2 (3.6)*	−2.1 (3.6)	2.9 (7.1)
Tb.Sp (mm)											
Baseline	0.243 (0.030)	0.189 (0.017)	0.190 (0.011)	0.357 (0.022)	0.316 (0.030)	0.336 (0.027)	0.297 (0.069)	0.218 (0.015)	0.209 (0.026)	0.460 (0.201)	0.373 (0.099)
Δ% non-radiated	−3.1 (6.0)	63.2 (34.7)*	17.3 (11.9)*	3.1 (12.0)	36.0 (34.5)*	23.1 (15.4)*	3.3 (11.4)	27.9 (18.3)*	22.5 (16.1)*	34.2 (24.8)*	4.0 (31.5)
Δ% radiated	5.8 (6.1)*	83.8 (27.9)*	33.3 (16.2)*	14.1 (13.2)*	52.9 (37.3)*	32.0 (20.0)*	24.0 (9.8)*	51.7 (30.9)*	36.3 (9.9)*	42.8 (34.3)*	2.9 (9.0)
Tb.N (1/mm)											
Baseline	4.39 (0.57)	5.34 (0.34)	5.37 (0.25)	2.89 (0.15)	3.25 (0.29)	3.05 (0.24)	3.61 (0.85)	4.64 (0.27)	4.86 (0.56)	2.64 (0.99)	2.96 (0.73)
Δ% non-radiated	−1.5 (8.8)	−34.7 (13.4)*	−12.1 (7.3)*	−1.8 (9.9)	−22.8 (16.8)*	−16.9 (9.4)*	−2.8 (9.5)	−19.9 (9.9)*	−15.9 (10.3)*	−23.0 (13.9)*	0.2 (21.0)
Δ% radiated	−6.7 (5.8)*	−42.7 (10.0)*	−21.8 (10.1)*	−11.2 (9.5)*	−31.6 (15.0)*	−21.9 (10.7)*	−18.4 (5.4)*	−31.2 (10.8)*	−24.8 (4.9)*	−25.4 (16.3)*	−0.3 (11.3)
Ct.Th (mm)											
Baseline	–[a]	0.206 (0.007)	0.210 (0.006)	–[a]	0.157 (0.007)	0.159 (0.010)	–[a]	0.188 (0.006)	0.188 (0.007)	0.430 (0.026)	0.462 (0.036)
Δ% non-radiated	–[a]	3.4 (4.6)	9.0 (5.2)*	–[a]	0.6 (6.7)	4.2 (5.3)	–[a]	−3.5 (8.9)	3.4 (2.7)*	9.7 (5.9)*	4.4 (6.6)
Δ% radiated	–[a]	5.1 (4.4)*	10.2 (5.5)*	–[a]	4.0 (6.6)	9.1 (3.8)*	–[a]	3.6 (9.1)	8.2 (2.5)*	8.5 (4.5)*	3.4 (3.7)*
Ct.A (mm^2)											
Baseline	–[a]	1.02 (0.03)	1.01 (0.05)	–[a]	0.85 (0.05)	0.83 (0.06)	–[a]	1.03 (0.08)	1.02 (0.09)	6.35 (0.45)	6.57 (0.22)
Δ% non-radiated	–[a]	2.5 (3.1)	8.4 (5.4)*	–[a]	1.2 (6.6)	2.9 (3.2)	–[a]	−3.7 (7.4)	3.1 (3.9)	6.1 (4.2)*	1.3 (8.6)
Δ% radiated	–[a]	4.5 (2.9)*	9.7 (4.7)*	–[a]	2.4 (6.4)	8.8 (3.7)*	–[a]	0.0 (6.8)	5.4 (4.6)*	4.4 (3.3)*	−0.2 (2.9)
Ma.A (mm^2)											
Baseline	–[a]	0.90 (0.065)	0.82 (0.072)	–[a]	1.34 (0.074)	1.34 (0.095)	–[a]	1.31 (0.077)	1.25 (0.142)	8.85 (0.67)	8.03 (1.3)
Δ% non-radiated	–[a]	6.8 (11.1)	−1.0 (11.2)	–[a]	2.1 (5.7)	−3.3 (4.0)	–[a]	5.0 (10.6)	3.7 (12.7)	−7.8 (4.7)*	6.2 (19.9)
Δ% radiated	–[a]	3.0 (8.9)	−1.1 (6.5)	–[a]	−2.8 (6.1)	−6.9 (3.0)*	–[a]	−1.1 (9.1)	−0.2 (9.5)	−6.0 (5.0)*	−1.6 (3.9)

Changes are reported as average relative difference (percent) between endpoint measurement and baseline [average relative difference = $\sum_{i=1}^{n}[((\text{endpoint}_i - \text{baseline}_i)/\text{baseline}_i)/n] \times 100$; n = sample number per group]. Asterisk (*) indicates significant difference between baseline and endpoint measurement.

[a] Ct.Th data unavailable for mouse control groups due to computer error.

the radiated limb. BAL mice lost $-18.3\% \pm 13.6\%$ of their BV/TV in the non-radiated limb but $-24.9\% \pm 17.7\%$ in the radiated limb. BL6 mice lost $-22.4\% \pm 28.9\%$ in the non-radiated limb while the radiated limb lost $-40.0\% \pm 19.1\%$. C3H mice lost $-39.1\% \pm 19.8\%$ in the non-radiated limb and $-51.4\% \pm 16.3\%$ in the radiated limb. Wistar rats lost $-31.5\% \pm 9.5\%$ in the non-radiated limb and $-36.3\% \pm 12.5\%$ in the radiated limb.

Sham BAL and C3H mice incurred BV/TV losses of $-10.4\% \pm 14.7\%$ and $-5.5\% \pm 4.7\%$, respectively, relative to baseline in the non-radiated limb. These effects were more pronounced in the radiated limb ($-18.9\% \pm 6.2\%$ for BAL and $-15.5\% \pm 7.9\%$ for C3H), although only significantly different for C3H. Sham BL6 mice increased BV/TV from baseline to endpoint in the non-radiated limb ($3.6\% \pm 9.9\%$) but lost BV/TV in the radiated limb ($-11.4\% \pm 12.4\%$). Sham-operated Wistar rats increased BV/TV from baseline to endpoint in both non-radiated ($7.3\% \pm 17.2\%$) and radiated limbs ($6.4\% \pm 12.2\%$).

Groups that displayed significant reductions in BV/TV between baseline and endpoint showed reductions in Tb.N between 12% and 43%, and increases in Tb.Sp between 17% and 84%. Longitudinal changes in Tb.Th were less than 10% for all groups except control C3H mice, and control and sham BL6 mice.

Changes relative to baseline were not as significant and more inconsistent for cortical bone, but general trends of increased Ct.Th and Ct.A were observed with greater increases in the radiated limbs. Ma.A was increasing non-significantly in the non-radiated limbs for all OVX mouse groups, while lesser increases or slight decreases were observed in the radiated limbs.

4. Discussion

In this study, we examined the effect of repeated *in vivo* micro-CT induced radiation exposure on bone architecture in healthy and ovariectomized groups of common inbred mice and rats. Examining the radiation effect in different species and different strains as well as its interactions with surgical treatment provides useful information for designing future *in vivo* studies where repeated radiation exposure may impact results.

There was no statistically significant interaction between radiation effect and surgical treatment within any group, which implies that the ovariectomy and sham-ovariectomy procedures do not render the bone more or less susceptible to radiation effects. In fact, for all three inbred mouse strains, the relative amounts of bone loss between OVX and sham groups are highly consistent with data previously observed in a cross-sectional study [28], where radiation effects are not a concern. Although the mice in the previous cross-sectional study were older (OVX at 16 weeks) than those used here, the consistency serves to illustrate the lack of interaction between radiation effect and surgical group.

From baseline to endpoint, the OVX groups had the greatest reductions in BV/TV, as well as the greatest increases in Tb.Sp and decreases in Tb.N. Tb.Th and cortical bone morphology was relatively unaffected. These patterns were the same for the sham groups, only with lower magnitudes. The relative bone loss between radiated and non-radiated limbs in each group is also a result of decreased BV/TV in the radiated limb accompanied by lower Tb.N and higher Tb.Sp, with little or no change in Tb.Th. Even for the control mouse groups, where BV/TV increases over time in the non-radiated limbs, growth was suppressed in the radiated limbs via increased Tb.Sp and lower Tb.N. This seems to indicate that both surgery-induced and radiation-induced bone loss is manifested through decreased connectivity and loss of thin trabecular elements, as opposed to gradual thinning of the entire structure.

It should be emphasized that the effects of OVX are not overshadowed by radiation effects for mouse strains with moderate to high bone volume densities. Ovariectomized C3H mice lost 50% of their BV/TV by week 5, while BL6 and BAL incurred 40% losses at week 5 and week 2, respectively (data not presented). The additional 10–20% relative losses between radiated and non-radiated limbs do not obscure these overall bone loss trends for the higher bone mass strains (BAL and C3H). The sham and control groups maintain much higher BV/TV levels than the OVX groups despite radiation effects (Fig. 1). This distinction is less clear for a lower bone mass strain like BL6. Since the baseline BV/TV at the proximal tibia is so low in this strain (less than 10%), the radiation effects on the sham animals reduce the BV/TV to levels very near those of the OVX group. Thus, it appears radiation should be more carefully considered for animals with low bone mass in the scanned region.

The precise mechanisms of radiation-induced bone loss are unclear. Just one of many possibilities is that damage to bone remodeling cells occurs, but we cannot distinguish here if the radiation effects are a result of decreased osteoblast activity or increased osteoclast activity. Radiation-induced effects on *in vitro* cultures of both cell types have been observed in the past at higher dose levels (2–10 Gy) [24,25,33,34], although no effects on cell viability were observed by Brouwers et al. when examining rats *in vivo* [26]. Further studies addressing this issue could make use of techniques like histology, histomorphometry, or cell viability staining to more closely examine whether osteoclast and osteoblast activity levels are affected by micro-CT radiation.

The radiation effects observed in the mice contrasts the lack of effect in the rats. This absence is consistent with previous findings in healthy rats [26], although a radiation effect may have been observed if the rats were examined over a longer time period and were subjected to additional scans (i.e., increased dosage). The more pronounced effect in mice compared to rats could be due to a number of factors. The mice used in this study were young ($\sim$12 weeks), and would have higher rates of bone formation than older animals [21,35]. These high bone formation rates, possibly coupled

with cellular changes mentioned previously, could play a role in the observed effects. Additionally, due to the higher resolution of the mouse scans, the radiation dose is over 40% higher for the mice than for the rats. At lower doses, mice may not incur such effects. It is also possible that rats as a species simply have a higher tolerance against radiation damage in bone than mice.

The effect of positioning the animal's limb in the scanner was not considered during this study. It is possible that this fixation could have an impact on the bone in the scanned limb, potentially confounding the radiation results. The authors do not expect this to be the case, as the leg is fixed for only a short time (∼12 min) without excessive stretching. To be sure, it would be prudent in future studies to account for this potential effect by fixing the contralateral limb in a similar position for an equal amount of time during each scanning interval.

The age of the control mice groups varied between 8 and 10 weeks of age, and studies have indicated that rapid changes in structure and density occur in mice near this age [21,36]. This would lead to some variation in skeletal behavior among the control group animals. However, since the observed radiation effect was similar for groups that lost and gained bone to various degrees, some slight variation within the control groups is likely acceptable without impacting the overall results.

The quantification of radiation effect as the relative difference between radiated and non-radiated limbs within the same animal at the end of a scanning protocol depends on the assumption that both limbs are not significantly different at the outset. In our preliminary work, groups of healthy BL6 and C3H mice did not significantly differ in baseline morphology at the proximal tibia metaphysis, supporting the assumption that handedness in mice is not a concern (data not published). Similar findings have been shown between left and right distal femurs in mice [37].

The radiation dose for this study was calculated using a thin-walled PEI tube surrounding an ionizing chamber probe. This differs from the calculations used in other micro-CT radiation studies [37,38] where the dose is calculated using a probe inside a 35 mm solid polymethyl methacrylate (PMMA) tube, which tends to result in a 50% dose reduction compared to the value measured in air. The method of using a solid PMMA tube extends from dose calculations in clinical CT measurements where large phantoms are used to represent the human body core. For micro-CT, particularly at the tibia, we do not have such a large volume of soft tissue surrounding the bone. Therefore the thin PEI we use is more representative of the dissipation of X-ray energy due to the skin at the mouse/rat tibia. Accordingly, the doses we report are slightly higher than those reported by previous studies, but are likely more representative of the true delivered dose.

In conclusion, this study indicates that the radiation dose administered during high-resolution *in vivo* micro-CT scanning has no effect on the bone structure of rats at the proximal tibia. Small, statistically significant effects on trabecular BV/TV (lower), Tb.Sp (higher), and Tb.N (lower) were consistently observed for skeletally immature C3H, BL6, and BAL mice. These effects are less than the observed effects due to mouse ovariectomy (e.g., 40–50% bone loss from baseline, depending on mouse strain), but should be carefully considered for strains with low bone volume at the measured site such as BL6. Radiation suppressed growth and induced losses in mice that were otherwise gaining bone mass, and further intensified losses in mice that were already losing bone. While it is not entirely clear whether the radiation effects in mice are due to increased bone resorption or suppressed bone formation, the practical end result is the same: repeatedly radiated limbs have lower net bone volume and a more sparsely connected trabecular network than their unscanned contralateral counterparts. Fortunately, the effect of the 712.4 mGy dose used on mice in this specific protocol does not overshadow bone loss effects due to ovariectomy in mice with sufficient bone mass at the measured site, and the radiation effects are not exacerbated by OVX or sham treatment. Comparison via paired *t*-test with an internal non-radiated control is a potential method to elucidate the effect of radiation exposure for any *in vivo* protocol. Radiation from *in vivo* micro-CT can have a small effect on trabecular bone in mice that are skeletally immature, and no detectable effect on aged rats. Thus, *in vivo* micro-CT remains poised to play an important role in bone-related research.

Acknowledgements

This work has been supported by grants from the Natural Sciences and Engineering Research Council of Canada (NSERC), the Canadian Institutes of Health Research (CIHR), the Canada Foundation for Innovation (CFI), the Alberta Heritage Foundation for Medical Research (AHFMR), and the Alberta Ingenuity Fund (AIF).

Conflict of interest

The authors have no conflict of interest.

References

[1] Ritman EL. Micro-computed tomography—current status and developments. Annu Rev Biomed Eng 2004;6:185–208.
[2] Rüegsegger P, Koller B, Müller R. A microtomographic system for the nondestructive evaluation of bone architecture. Calcif Tissue Int 1996;58(1):24–9.
[3] Boyd SK, Kuhn M, Moser S, Krauze P, Klinck RJ, Mattmann C, et al. Three-dimensional image registration for longitudinal site-specific measure of bone adaptation. In: Proceedings of 14th European Society of Biomechanics Conference, 's-Hertogenbosch, Netherlands. 2004. p. 514.
[4] Boyd SK, Mattmann C, Kuhn A, Müller R, Gasser JA. A novel approach for monitoring and predicting bone microstructure in osteoporosis. In: 26th American Society of Bone and Mineral Research Annual Meeting, Seattle, USA. J Bone Miner Res 2004;S236–7.

[5] Mattmann C, Kuhn A, Gasser JA, Müller R, Boyd SK. Site specific micro-architectural bone changes with in vivo computed tomography. In: 16th International Bone Densitometry Workshop, Annecy, France. 2004. p. 84.
[6] Waarsing JH, Day JS, van der Linden JC, Ederveen AG, Spanjers C, De Clerck N, et al. Detecting and tracking local changes in the tibiae of individual rats: a novel method to analyse longitudinal in vivo micro-CT data. Bone 2004;34(1):163–9.
[7] Kleerekoper M, Villanueva AR, Stanciu J, Rao DS, Parfitt AM. The role of three-dimensional trabecular microstructure in the pathogenesis of vertebral compression fractures. Calcif Tissue Int 1985;37(6):594–7.
[8] Peacock M, Turner CH, Econs MJ, Foroud T. Genetics of osteoporosis. Endocr Rev 2002;23(3):303–26.
[9] Ray NF, Chan JK, Thamer M, Melton 3rd LJ. Medical expenditures for the treatment of osteoporotic fractures in the United States in 1995: report from the National Osteoporosis Foundation. J Bone Miner Res 1997;12(1):24–35.
[10] Moore R, Mao Y, Zhang J, Clarke K. Economic burden of illness in Canada. Ottawa, Canada: Minister of Public Works and Government Services Canada; 1993.
[11] Cauley JA, Thompson DE, Ensrud KC, Scott JC, Black D. Risk of mortality following clinical fractures. Osteoporos Int 2000;11(7):556–61.
[12] Laib A, Kumer JL, Majumdar S, Lane NE. The temporal changes of trabecular architecture in ovariectomized rats assessed by micro-CT. Osteoporos Int 2001;12(11):936–41.
[13] Lane NE, Haupt D, Kimmel DB, Modin G, Kinney JH. Early estrogen replacement therapy reverses the rapid loss of trabecular bone volume and prevents further deterioration of connectivity in the rat. J Bone Miner Res 1999;14(2):206–14.
[14] Kinney JH, Haupt DL, Balooch M, Ladd AJ, Ryaby JT, Lane NE. Three-dimensional morphometry of the L6 vertebra in the ovariectomized rat model of osteoporosis: biomechanical implications. J Bone Miner Res 2000;15(10):1981–91.
[15] Kneissel M, Boyde A, Gasser JA. Bone tissue and its mineralization in aged estrogen-depleted rats after long-term intermittent treatment with parathyroid hormone (PTH) analog SDZ PTS 893 or human PTH(1–34). Bone 2001;28(3):237–50.
[16] Alexander JM, Bab I, Fish S, Müller R, Uchiyama T, Gronowicz G, et al. Human parathyroid hormone 1–34 reverses bone loss in ovariectomized mice. J Bone Miner Res 2001;16(9):1665–73.
[17] Baltzer AW, Whalen JD, Wooley P, Latterman C, Truchan LM, Robbins PD, et al. Gene therapy for osteoporosis: evaluation in a murine ovariectomy model. Gene Ther 2001;8(23):1770–6.
[18] Wu J, Wang XX, Takasaki M, Ohta A, Higuchi M, Ishimi Y. Cooperative effects of exercise training and genistein administration on bone mass in ovariectomized mice. J Bone Miner Res 2001;16(10):1829–36.
[19] Kasukawa Y, Stabnov L, Miyakoshi N, Baylink DJ, Mohan S. Insulin-like growth factor. I. Effect on the number of osteoblast progenitors is impaired in ovariectomized mice. J Bone Miner Res 2002;17(9):1579–87.
[20] Turner CH, Hsieh YF, Müller R, Bouxsein ML, Rosen CJ, McCrann ME, et al. Variation in bone biomechanical properties, microstructure, and density in BXH recombinant inbred mice. J Bone Miner Res 2001;16(2):206–13.
[21] Beamer WG, Donahue LR, Rosen CJ, Baylink DJ. Genetic variability in adult bone density among inbred strains of mice. Bone 1996;18(5):397–403.
[22] Mitchell MJ, Logan PM. Radiation-induced changes in bone. Radiographics 1998;18(5):1125–36 [quiz 1242–3].
[23] Dudziak ME, Saadeh PB, Mehrara BJ, Steinbrech DS, Greenwald JA, Gittes GK, et al. The effects of ionizing radiation on osteoblast-like cells in vitro. Plast Reconstr Surg 2000;106(5):1049–61.
[24] Gal TJ, Munoz-Antonia T, Muro-Cacho CA, Klotch DW. Radiation effects on osteoblasts in vitro: a potential role in osteoradionecrosis. Arch Otolaryngol Head Neck Surg 2000;126(9):1124–8.
[25] Matsumura S, Jikko A, Hiranuma H, Deguchi A, Fuchihata H. Effect of X-ray irradiation on proliferation and differentiation of osteoblast. Calcif Tissue Int 1996;59(4):307–8.
[26] Brouwers JE, van Rietbergen B, Huiskes R. No effects of in vivo micro-CT radiation on structural parameters and bone marrow cells in proximal tibia of wistar rats detected after eight weekly scans. J Orthop Res 2007;25:1325–32.
[27] Judex S, Chung H, Torab A, Xie L, Rubin C, Donahue LR, et al. Micro-CT induced radiation does not exacerbate disuse related bone loss. Washington, DC: Orthopaedic Research Society; 2005.
[28] Bouxsein ML, Myers KS, Shultz KL, Donahue LR, Rosen CJ, Beamer WG. Ovariectomy-induced bone loss varies among inbred strains of mice. J Bone Miner Res 2005;20(7):1085–92.
[29] Judex S, Garman R, Squire M, Donahue LR, Rubin C. Genetically based influences on the site-specific regulation of trabecular and cortical bone morphology. J Bone Miner Res 2004;19(4):600–6.
[30] Iwaniec UT, Yuan D, Power RA, Wronski TJ. Strain-dependent variations in the response of cancellous bone to ovariectomy in mice. J Bone Miner Res 2006;21(7):1068–74.
[31] Li CY, Schaffler MB, Wolde-Semait HT, Hernandez CJ, Jepsen KJ. Genetic background influences cortical bone response to ovariectomy. J Bone Miner Res 2005;20(12):2150–8.
[32] Boyd SK, Davison P, Müller R, Gasser JA. Monitoring individual morphological changes over time in ovariectomized rats by in vivo micro-computed tomography. Bone 2006;39(4):854–62.
[33] Scheven BA, Burger EH, Kawilarang-de Haas EW, Wassenaar AM, Nijweide PJ. Effects of ionizing irradiation on formation and resorbing activity of osteoclasts in vitro. Lab Invest 1985;53(1):72–9.
[34] Scheven BA, Wassenaar AM, Kawilarang-de Haas EW, Nijweide PJ. Direct and indirect radiation effects on osteoclast formation in vitro. Bone Miner 1987;2(4):291–300.
[35] Sheng MH, Baylink DJ, Beamer WG, Donahue LR, Rosen CJ, Lau KH, et al. Histomorphometric studies show that bone formation and bone mineral apposition rates are greater in C3H/HeJ (high-density) than C57BL/6J (low-density) mice during growth. Bone 1999;25(4):421–9.
[36] Glatt V, Canalis E, Stadmeyer L, Bouxsein ML. Age-related changes in trabecular architecture differ in female and male C57BL/6J mice. J Bone Miner Res 2007;22(8):1197–207.
[37] Judex S, Chung H, Torab A, Xie L, Rubin CT, Donahue LR, et al. Micro-CT induced radiation does not exacerbate disuse related bone loss. In: Proceedings of the 51st Annual Meeting of the Orthopaedic Research Society. 2005.
[38] Brouwers JEM, van Rietbergen B, Huiskes R. In vivo micro-CT radiation does not affect bone structure in rats. In: Proceedings of the 52nd Annual Meeting of the Orthopaedic Research Society. 2006.